

See discussions, stats, and author profiles for this publication at: <https://www.researchgate.net/publication/50865097>

Briarane Diterpenes Diminish COX-2 Expression in Human Colon Adenocarcinoma Cells

ARTICLE *in* JOURNAL OF NATURAL PRODUCTS · MARCH 2011

Impact Factor: 3.8 · DOI: 10.1021/np100775a · Source: PubMed

CITATIONS

8

READS

28

7 AUTHORS, INCLUDING:



[Amanda Leigh Waters](#)

NCI-Frederick

11 PUBLICATIONS 69 CITATIONS

[SEE PROFILE](#)



[Russell B. Williams](#)

Sequoia Sciences, Inc.

29 PUBLICATIONS 380 CITATIONS

[SEE PROFILE](#)



[Naveena B Janakiram](#)

University of Oklahoma Health Sciences Cen...

67 PUBLICATIONS 983 CITATIONS

[SEE PROFILE](#)



[Chinthalapally V Rao](#)

University of Oklahoma Health Sciences Cen...

267 PUBLICATIONS 11,430 CITATIONS

[SEE PROFILE](#)

Briarane Diterpenes Diminish COX-2 Expression in Human Colon Adenocarcinoma Cells

P. Matthew Joyner,^{†,‡} Amanda L. Waters,[†] Russell B. Williams,[†] Douglas R. Powell,[†] Naveena B. Janakiram,[§] Chinthalapally V. Rao,[§] and Robert H. Cichewicz^{*,†,⊥}

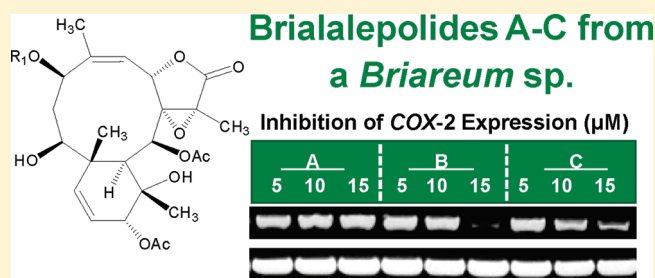
[†]Natural Products Discovery Group, Department of Chemistry and Biochemistry, Stephenson Life Sciences Research Center, 101 Stephenson Parkway, University of Oklahoma, Norman, Oklahoma 73019, United States

[§]Department of Medicine, University of Oklahoma Cancer Institute, University of Oklahoma Health Sciences Center, Oklahoma City, Oklahoma 73104, United States

[⊥]Graduate Program in Ecology and Evolutionary Biology, University of Oklahoma, Norman, Oklahoma 73019, United States

S Supporting Information

ABSTRACT: Exploration of a soft coral (*Briareum* sp.) from Vanuatu led to the isolation of three new briaranes, designated brialepolides A (1), B (2), and C (3). Compounds 2 and 3 reduced the expression of COX-2 in human colon adenocarcinoma cells, as well as in murine macrophage cells. This is significant because the metabolic products of COX-2 have been implicated in the pathogenesis of colon cancer and other diseases.



Briarane diterpenes are a unique class of marine-derived secondary metabolites possessing a bicyclo[4.4.0] skeleton with a fused γ -lactone. Since the first briarane diterpene, briarein A, was reported in 1977 from a gorgonian coral by Burks and colleagues at the University of Oklahoma,¹ more than 500 related metabolites have been described from corals and other marine invertebrates.^{2–5} Notable features of the structural diversity within this family of compounds include functionalization, ring-opening/closure, and epimerization at all 20 positions of the briarane carbon skeleton. The extraordinary structural variation has made these metabolites an attractive subject for assessing how their naturally occurring chemical variation influences their biological activities. For example, briaranes have been reported to possess anti-inflammatory and antiviral effects, as well as cytotoxicity against several cancer cell lines.^{2–4}

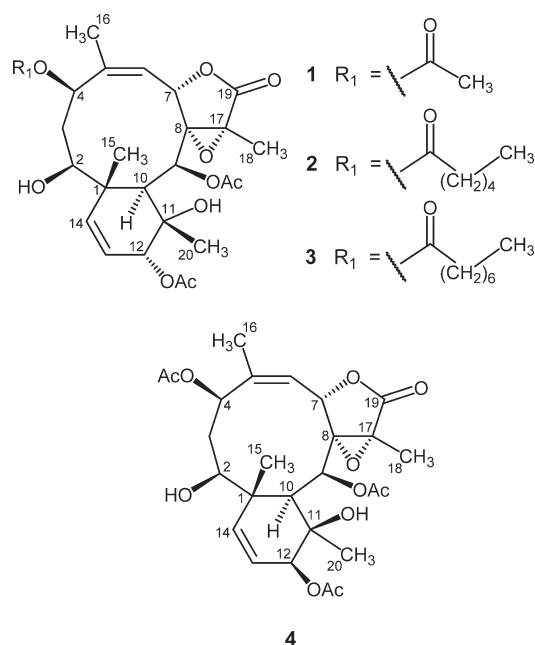
Colorectal cancer is one of the most common and deadly forms of cancer, with approximately 50 000 people in the United States estimated to succumb to the disease in 2010.⁶ Although the molecular pathology of colon cancer is not fully understood, research has demonstrated that the cyclooxygenase 2 gene (COX-2) is upregulated in the majority of colorectal tumors.^{7,8} COX-2 catalyzes the transformation of arachidonic acid to prostaglandin PGG₂, which is then converted to prostaglandin PGH₂. The increased production of COX-2 is believed to contribute to tumorigenesis through a signal cascade mechanism that is activated by prostaglandins. The metabolic products of COX-2 are believed to play important roles in facilitating tumor-promoting activities such as enhancing angiogenesis and inhibiting apoptosis.^{7,8} Consequently, decreasing the activity

of COX-2 through direct inhibition or by suppressing COX-2 expression have been proposed as potential chemopreventative approaches for cancer therapy.^{7,8} In this report, we describe three new briarane diterpenes (1–3) that are cytotoxic to human colon adenocarcinoma cells and show that these secondary metabolites are also capable of altering COX-2 expression.

The CH₂Cl₂–MeOH (1:1) extract of *Briareum* sp. was partitioned between H₂O and EtOAc. The EtOAc layer was retained and the solvent removed under vacuum. The resulting organic residue was analyzed by gradient C₁₈ HPLC, which revealed three major metabolites that were targeted for isolation. Compound 1 eluted first from the C₁₈ column, and it exhibited a pseudomolecular ion [M + Na]⁺ of m/z of 545.2004 by HRESIMS. This corresponded to a molecular formula of C₂₆H₃₄NaO₁₁ for 1. Inspection of the ¹³C NMR data for 1 (Table 1) revealed a total of 26 unique carbon atoms, which included four carbonyls (δ_C 168.3, 169.8, 170.3, and 170.4), four olefinic carbons (δ_C 121.9, 122.5, 142.0, and 144.2), and eight sp^3 -hybridized carbons attached to oxygens (δ_C 64.8, 65.1, 71.3, 72.4, 72.8, 73.5, 73.6, and 77.4). The ¹J_{H–C} HSQC data for the remaining carbon resonances appearing between δ_C 9.7 and 48.2 enabled us to confirm that seven of the carbons were methyls (δ_C 9.7, 14.0, 20.9, 21.0, 21.2, 21.6, and 26.5). Given the biogenic source of compound 1, both the HRESIMS and HSQC data were consistent with what we expected for briarane-diterpene-type

Received: October 25, 2010

Published: March 25, 2011



metabolites that are commonly encountered in this genus of corals.^{9–11} We observed notable similarities between our data and those reported by Wu et al. for briaexcavatulide S (**4**).¹² Consequently, we focused our attention on using the basic briarane diterpene scaffold of **4** as a convenient tool for accelerating the structural characterization of **1**.

While all of the proton and carbon resonances in the cyclodecane and fused γ -lactone ring portions of **1** closely matched the data for **4**, we noted some modest differences among the carbon resonances in the vicinity of the hexene ring system. For example, we observed that C-20 in **1** resonated at δ_C 21.2, whereas in **4** this carbon was reported to appear at δ_C 28.8 (Δ –7.6 ppm). Other carbon chemical shifts in the cyclohexene system that varied between **1** and **4** included C-1 (Δ 0.2 ppm), C-10 (Δ –1.1 ppm), C-11 (Δ –1.5 ppm), C-12 (Δ –1.8 ppm), C-13 (Δ 3.1 ppm), and C-14 (Δ –3.2 ppm). In light of these differences in the spectroscopic data between **1** and **4**, we reasoned that the compounds must share similar relative configurations that vary at only one or more asymmetric centers within the cyclohexene system. Using NOESY to probe this portion of **1** (Supporting Information, Table S1), we observed a series of informative correlations that enabled us to investigate the relative configuration of the asymmetric carbons C-1, C-10, C-11, and C-12. Whereas the H-15 methyl protons exhibited NOE correlations with H-14 and H-20, the H-10 proton was only correlated with H-2. The H-20 protons exhibited additional correlations that included H-9, H-12, and OH-11. An additional set of correlations were detected between OH-11 and H-9 and H-12. In consideration of these data, the relative configuration of C-11 and C-12 in compound **1** was the opposite of what had been reported for compound **4**.

While in the process of establishing the relative configuration of **1**, we were successful in preparing crystals of this metabolite for X-ray diffraction studies. An ORTEP illustration generated from these data is shown in Figure 1. The data from this experiment supported the proposed relative configuration of **1** and enabled us to unequivocally determine the absolute configuration of the metabolite using the Hooft method¹³ as 1S,2S,4R,7S,8S,9S,10S,11S,12R,17R.

Table 1. ^{13}C NMR Data (CDCl_3) for Briaralepolides **A** (**1**), **B** (**2**), and **C** (**3**)

position	δ_C , number of attached protons ^a		
	1 ^b	2 ^c	3 ^c
1	48.2, C	48.2, C	48.2, C
2	77.4, CH	77.5, CH	77.5, CH
3	40.1, CH ₂	40.2, CH ₂	40.2, CH ₂
4	72.8, CH	72.5, CH	72.5, CH
5	144.2, C	144.3, C	144.4, C
6	122.5, CH	122.4, CH	122.4, CH
7	73.6, CH	73.6, CH	73.6, CH
8	71.3, C	71.4, C	71.4, C
9	65.1, CH	65.2, CH	65.2, CH
10	44.6, CH	44.7, CH	44.7, CH
11	72.4, C	72.6, C	72.6, C
12	73.5, CH	73.5, CH	73.5, CH
13	121.9, CH	122.1, CH	122.0, CH
14	142.0, CH	141.9, CH	142.0, CH
15	14.0, CH ₃	14.1, CH ₃	14.1, CH ₃
16	26.5, CH ₃	26.5, CH ₃	26.5, CH ₃
17	64.8, C	64.9, C	64.9, C
18	9.7, CH ₃	9.7, CH ₃	9.7, CH ₃
19	170.4, C	170.4, C	170.4, C
20	21.2, CH ₃	21.2, CH ₃	21.2, CH ₃
1'		173.2, C	173.1, C
2'		34.2, CH ₂	34.2, CH ₂
3'		24.5, CH ₂	24.8, CH ₂
4'		31.2, CH ₂	29.0, CH ₂
5'		22.3, CH ₂	28.9, CH ₂
6'		13.9, CH ₃	31.6, CH ₂
7'			22.6, CH ₂
8'			14.1, CH ₃
4-OCOCH ₃	170.3, C		
4-OCOCH ₃	21.0, CH ₃		
9-OCOCH ₃	168.3, C	168.3, C	168.3, C
9-OCOCH ₃	21.6, CH ₃	21.6, CH ₃	21.6, CH ₃
12-OCOCH ₃	169.8, C	169.8, C	169.8, C
12-OCOCH ₃	20.9, CH ₃	20.9, CH ₃	20.9, CH ₃

^a Determined by HSQC experiment. ^b Data for ^{13}C NMR determined at 125 MHz. ^c Data for ^{13}C NMR determined at 100 MHz.

The HRESIMS analysis of compound **2** provided a pseudo-molecular ion $[\text{M} + \text{Na}]^+$ at m/z 601.2616 that was consistent with a molecular formula of $\text{C}_{30}\text{H}_{42}\text{NaO}_{11}$. Upon examination of the ^1H NMR data, it became apparent that compound **2** was structurally similar to **1** (Tables 1 and 2). Two notable changes in the ^1H NMR spectrum of **2** were the replacement of an acetate methyl singlet in **1** by a methyl triplet (δ_H 0.9, t, J = 7.0 Hz) in **2** and the observation of eight new protons at δ_H 2.32 (t, J = 7.5 Hz, 2H), 1.64 (m, 2H), and 1.32 (m, 4H). In addition, the ^{13}C NMR (Table 1) and ^1H - ^{13}C HSQC spectra of **2** exhibited four new methylene carbon resonances at δ_C 22.3, 24.5, 31.2, and 34.2 that accounted for all eight of the new protons. Given the substantial quantity of **2** that was available (>500 mg), we took advantage of the opportunity to perform a ^{13}C - ^{13}C INADEQUATE experiment (Supporting Information, Figure S1). On

the basis of the results from this study, we concluded that the aforementioned methylenes were part of a pendant hexanoate that began with an ester carbonyl (δ_C 173.2) and terminated in a methyl group (δ_C 13.9). HMBC and NOESY data confirmed that the only difference between compounds **1** and **2** was the

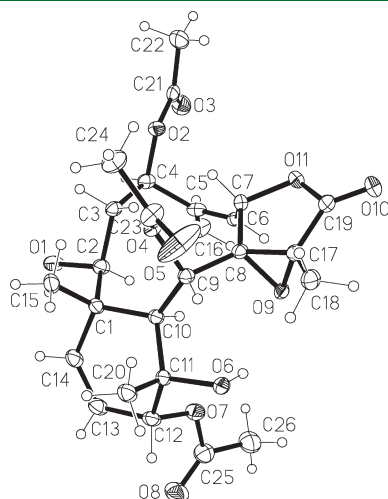


Figure 1. ORTEP drawing for the X-ray crystal structure of **1**.

substitution of the C-4 acetate with hexanoate. We propose that the absolute configuration of **2** is also 1*S*,2*S*,4*R*,7*S*,8*S*,9*S*,10*S*,11*S*,12*R*,17*R* on the basis of its shared biogenic origins and similar specific rotation data ($[\alpha]^{21}_D$ -110 and -101 for **1** and **2**, respectively).

Compound **3** yielded a pseudomolecular ion (HRESIMS $[M + Na]^+$) at m/z 629.2938 consistent with a molecular formula of $C_{32}H_{46}NaO_{11}$. Compared to **2**, the molecular formula of **3** represented an increase of C_2H_4 , which we speculated was due to the addition of two methylenes. Examination of the 1H NMR integration data for **3** revealed four new protons in the region spanning δ_H 1.28 to 1.31 (Table 2). Data from an HSQC experiment confirmed that these protons were associated with two new methylenes (δ_C 28.9 and 29.0), while HMBC correlations established that these carbons were situated among a group of four other methylenes (δ_C 22.6, 24.8, 31.6, and 34.2), a carbonyl (δ_C 173.1), and a methyl group (δ_C 14.1) (Supporting Information, Table S3). Together, these carbons formed an octanoate ester. The only difference in this new metabolite was that **3** bore a C-4 octanoate ester, whereas **1** and **2** possessed C-4 acetate and hexanoate groups, respectively. We propose that the absolute configuration of **3** is 1*S*,2*S*,4*R*,7*S*,8*S*,9*S*,10*S*,11*S*,12*R*,17*R*.

Compounds **1**–**3** were tested for cytotoxicity against Caco-2 cells, which were derived from a human epithelial colon adenocarcinoma.

Table 2. 1H NMR Data ($CDCl_3$) for Brialepolides A (**1**), B (**2**), and C (**3**)

position	δ_H , multiplicity (J in Hz)		
	1 ^a	2 ^b	3 ^a
2	3.25, dd (5.5, 7.0)	3.27, dd (5.0, 7.0)	3.26, t (7.5)
3a	2.00, m	2.00, m	2.00, m
3b	2.84, t (13.0)	2.84, dd (13.0, 14.3)	2.85, dd (12.7, 14.3)
4	5.16, ddd (1.0, 5.5, 13.0)	5.17, dd (5.0, 7.0, 13.0)	5.17, ddd (1.0, 5.5, 12.7)
6	5.41, dt (1.3, 9.5)	5.41, dt (1.3, 9.5)	5.40, dt (1.5, 9.5)
7	5.78, d (9.5)	5.78, d (9.5)	5.78, d (9.5)
9	5.92, d (4.0)	5.92, d (3.8)	5.92, d (4.0)
10	2.46, d (4.0)	2.47, d (3.8)	2.47, d (4.0)
12	4.73, d (6.0)	4.75, d (6.0)	4.74, d (6.0)
13	5.96, dd (6.0, 10.3)	5.97, dd (6.0, 10.3)	5.96, dd (6.0, 10.3)
14	5.89, d (10.3)	5.89, d (10.3)	5.89, d (10.3)
15	1.13, s	1.13, s	1.13, s
16	2.04, d (1.3)	2.05, d (1.3)	2.05, d (1.5)
18	1.67, s	1.69, s	1.68, s
20	1.21, s	1.22, s	1.22, s
2'		2.32, t (7.5)	2.32, t (7.5)
3'		1.64, m	1.62, m
4'		1.32, m	1.31, m
5'		1.32, m	1.31, m
6'		0.90, t (7.0)	1.29, m
7'			1.28, m
8'			0.88, t (7.0)
4-OCOCH ₃	2.08, s		
9-OCOCH ₃	2.24, s	2.24, s	2.24, s
12-OCOCH ₃	2.06, s	2.07, s	2.06, s
2-OH	2.14, d (5.5)	4.87, br s	2.63, br s
11-OH	2.38, s	2.39, br s	2.39, br s

^aData for 1H NMR determined at 500 MHz. ^bData for 1H NMR determined at 400 MHz.

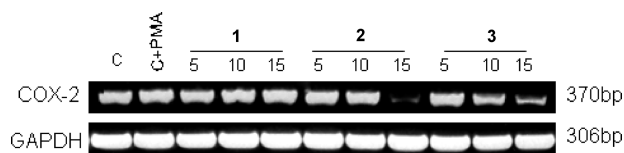


Figure 2. *COX-2* expression profiles in RAW 264.7 cells treated with brialalepolides A (1), B (2), and C (3). Decreases in PMA-induced *COX-2* mRNA levels were observed in cells treated with brialalepolides B and C, but brialalepolide A showed no effect. Expression of *GAPDH* was used as a positive control.

All three compounds exhibited dose-dependent cytotoxicity against Caco-2 cells over a range of 5–30 μM (Supporting Information, Figure S2). At the maximum dose of 30 μM , considerable cytotoxicity was observed (i.e., $\sim 75\%$ reduction in cell viability for compound 3), with 2 and 3 being more potent than 1. At concentrations of 30, 20, and 15 μM , for compounds 1, 2, and 3, respectively, an approximate 50% decrease in cell viability was observed. Compounds 1–3 were also investigated for their abilities to modulate the expression of the *COX-2* gene. While compound 1 appeared inactive at the concentrations tested, compounds 2 and 3 both substantially reduced levels of *COX-2* mRNA in Caco-2 cells (Supporting Information, Figure S23). We also observed decreased *COX-2* expression in RAW 264.7 cells (Figure 2). These cells are derived from mouse macrophages and are used for testing the effects of drugs on inflammation pathways.¹⁴ These data support the idea that briaranes such as 1–3 might be interesting candidates for therapeutic consideration as dual-acting cancer cell cytotoxins and inflammatory response inhibitors.

EXPERIMENTAL SECTION

General Experimental Procedures. Optical rotations were measured on a Rudolph Research Autopol III automatic polarimeter. NMR data were obtained on Varian VNMR spectrometers (400 and 500 MHz for ^1H , 100 and 125 MHz for ^{13}C) with broad band and triple resonance probes at $20 \pm 0.5^\circ\text{C}$. Electrospray-ionization mass spectrometry data were performed on a LCT Premier (Waters Corp.) time-of-flight instrument. HPLC separations were performed on a Shimadzu system using a SCL-10A VP system controller and Gemini 5 μm C_{18} column (110 Å, 250×21.2 mm) with a flow rate of 10 mL/min. X-ray diffraction data were collected on a Bruker-AXS with an APEX CCD area detector with a Mo X-ray source. All solvents used were of ACS grade or better.

Animal Material and Sample Preparation. The *Briareum* sp. used for this project was obtained from the National Cancer Institute's Natural Products Repository of marine invertebrates (identification number C020997-A/20). The sample was collected in November 2000 in the Republic of Vanuatu at a depth of 10 m and was brown in color, with a magenta interior. The organism was not a recognized species by the taxonomist. A voucher specimen is stored at the Department of Invertebrate Biology at the Smithsonian Institution under the number 0CDN7627 and is available for taxonomic investigation via the NCI. Materials were frozen within 2 h of collection and were maintained frozen until workup. The whole sample was crushed with dry ice and milled, followed by sublimation of the dry ice at -40°C . The remaining powder was then stirred at 4°C with approximately a liter of deionized H_2O for 4 h. The supernatant solution was removed via continuous centrifugation at room temperature, and the pellet was collected on Whatman 3 mm paper. The pellet, paper, and aqueous extract were lyophilized to dryness. The aqueous extract was bottled and stored at -20°C . The dried pellet and paper were then extracted at room temperature overnight using 1 L of a 1:1 (v/v) mixture of MeOH

and CH_2Cl_2 . The organic liquid was drained off under vacuum, the pellet was washed with approximately 100 mL of MeOH, and the solvent was removed from this combined organic extract *in vacuo*. This extract was stored at -20°C until it was used in this study.

Purification of the Brialalepolides A–C (1–3). The extract was suspended in H_2O and partitioned against EtOAc. The EtOAc-soluble material (4 g) was prepared for HPLC by passing it through a C_{18} SPE cartridge and eluting it with MeOH. The extract was subjected to preparative-scale HPLC by passing the material over a C_{18} column with a mobile phase of 40–100% CH_3CN – H_2O over 50 min. The first substantial peak to elute from the column was pure 1 (965 mg). The second major peak to elute from the preparative HPLC was determined by HRESIMS and ^1H NMR to be a mixture of structurally related metabolites. This mixture was further purified by subjecting the material to a second round of C_{18} HPLC with an isocratic elution scheme utilizing 68% CH_3CN in H_2O . This provided 520 mg of 2. The third fraction to elute from preparative HPLC (96 mg) was determined to be a mixture, and it was subsequently purified by C_{18} HPLC with a 45–65% CH_3CN – H_2O gradient, which yielded 54 mg of 3.

Brialalepolide A (1): colorless, crystalline solid (MeOH); mp $216\text{--}225^\circ\text{C}$; $[\alpha]_D^{21} -110$ (c 0.001, acetone); ^1H NMR, see Table 2; ^{13}C NMR see Table 1; HRESIMS m/z 545.2004 $[\text{M} + \text{Na}]^+$ (calcd for $\text{C}_{26}\text{H}_{34}\text{NaO}_{11}$, 545.1993).

Brialalepolide B (2): white powder; $[\alpha]_D^{21} -101$ (c 0.0024, CHCl_3); ^1H NMR, see Table 2; ^{13}C NMR see Table 1; HRESIMS m/z 601.2616 $[\text{M} + \text{Na}]^+$ (calcd for $\text{C}_{30}\text{H}_{42}\text{NaO}_{11}$, 601.2619).

Brialalepolide C (3): white powder; $[\alpha]_D^{21} -102$ (c 0.0024, CHCl_3); ^1H NMR, see Table 2; ^{13}C NMR see Table 1; HRESIMS m/z 629.2938 $[\text{M} + \text{Na}]^+$ (calcd for $\text{C}_{32}\text{H}_{46}\text{NaO}_{11}$, 629.2932).

Brialalepolide A (1) X-ray Spectroscopy. A colorless block-shaped crystal from MeOH of dimensions $0.37 \times 0.28 \times 0.24$ mm was selected for structural analysis. Intensity data for this compound were collected using a diffractometer with graphite-monochromated Mo $\text{K}\alpha$ radiation ($\lambda = 0.71073$ Å). The sample was cooled to 100 K. Cell parameters were determined from a nonlinear least-squares fit of 8427 peaks in the range $2.21^\circ < \theta < 28.29^\circ$. A total of 11 814 data were measured in the range $2.21^\circ < \theta < 26.00^\circ$ using ω oscillation frames. The data were corrected for absorption by the semiempirical method, giving minimum and maximum transmission factors of 0.961 and 0.979. The data were merged to form a set of 5239 independent data with $R(\text{int}) = 0.0258$ and a coverage of 100%.

The monoclinic space group $P2_1$ was determined by systematic absences and statistical tests and verified by subsequent refinement. The structure was solved by direct methods and refined by full-matrix least-squares methods on F^2 . The positions of hydrogens bonded to carbons were initially determined by geometry and refined by a riding model. Hydrogen atoms bonded to oxygens were located on a difference map, and their positions were refined independently. Non-hydrogen atoms were refined with anisotropic displacement parameters. Hydrogen atom displacement parameters were set to 1.2 (1.5 for methyl) times the displacement parameters of the bonded atoms. A total of 340 parameters were refined against one space group restraint and 5239 data to give $wR(F^2) = 0.0766$ and $S = 1.005$ for weights of $w = 1/[\sigma^2(F^2) + (0.0360P)^2 + 0.2800P]$, where $P = [F_o^2 + 2F_c^2]/3$. The final $R(F)$ was 0.0331 for the 4977 observed $[F > 4\sigma(F)]$ data. The largest shift/su was 0.000 in the final refinement cycle. The final difference map had maxima and minima of 0.177 and -0.175 e/Å³, respectively. Further crystallographic data and structure refinement for brialalepolide A (1) (Table S4), a structure with atom numbering used for X-ray experiments (Figure S24) and a CIF file are available in the Supporting Information.

Cytotoxicity Assay. The Caco-2 human colon cancer cell line was obtained from the American Type Culture Collection and maintained in MEM medium supplemented with 10% heat-inactivated fetal bovine serum and antibiotics (100 units/mL penicillin G and 100 $\mu\text{g}/\text{mL}$ streptomycin).

Cells were incubated at 37 °C in a humidified atmosphere with 95% air and 5% CO₂. Cultures at 60–70% confluence were used for all experiments, and each set of experiments was run three times. A 5 mg/mL stock solution of each compound was prepared in DMSO. The cytotoxic effect of the compounds against Caco-2 cell viability was performed using the trypan blue exclusion method.¹⁵ Exponentially growing Caco-2 were seeded in complete medium along with compound, and after 24 h, floating and adherent cells were collected and suspended in 25 μ L of PBS. Cells were mixed with 0.4% trypan blue, and the stained and unstained cells were counted using a hemacytometer.

COX-2 Expression Assay. RAW 264.7 cell monolayers were stimulated with phorbol 12-myristate 13-acetate (PMA) to induce COX-2 expression and were co-incubated with varying doses (0–15 μ M) of each compound for 24 h. Isolation of total cellular RNA was performed using a Totally RNA Kit (Ambion) as per the manufacturer's instructions. Equal quantities of RNA were used as templates for preparing cDNA by employing a SuperScript Reverse Transcriptase (Invitrogen). PCR amplification of COX-2 cDNA fragments was performed using the Taq Polymerase Master Mix (Qiagen, Inc.) with the following conditions: denaturation at 94 °C for 3 min followed by 35 cycles of 94 °C for 30 s, 56 °C for 1 min, 78 °C for 30 s. The following oligonucleotide primer sequences were used: 5'-AGACAGATCATTGCTGGCCGGGT-3' (sense) and 5'-TGCAGATGAGAGACTGAATTGAGG-3' (antisense). The PCR products were visualized and photographed under UV illumination.

■ ASSOCIATED CONTENT

S Supporting Information. X-ray spectroscopy data for compound 1, HRESIMS and NMR (¹H and ¹³C NMR, HSQC, HMBC, COSY, and NOESY) data for compounds 1–3, and supporting methods and data for the Caco-2 cytotoxicity and COX-2 expression assays. This information is available free of charge via the Internet at <http://pubs.acs.org>.

■ AUTHOR INFORMATION

Corresponding Author

*Tel: (405) 325-6969. Fax: (405) 325-6111. E-mail: rhchewicz@ou.edu

Present Addresses

[†]Department of Chemistry, Natural Science Division, Pepperdine University, Malibu, CA 90263, USA.

■ ACKNOWLEDGMENT

Financial support for this project was provided by the University of Oklahoma Department of Chemistry and Biochemistry and the College of Arts and Sciences. The X-ray diffractometer was purchased through a grant from the NSF (CHE-0130835), and the 400 MHz NMR spectrometer was obtained through a NSF CRIF MU grant (CHE-0639199). The author's express their gratitude to D. Newman for information regarding the collection and extraction of the coral specimen.

■ REFERENCES

- (1) Burks, J. E.; Van der Helm, D.; Chang, C. Y.; Ciereszko, L. S. *Acta Crystallogr., Sect. B: Struct. Crystallogr. Cryst. Chem.* **1977**, B33, 704–709.
- (2) Sung, P.-J.; Sheu, J.-H.; Wang, W.-H.; Fang, L.-S.; Chung, H.-M.; Pai, C.-H.; Su, Y.-D.; Tsai, W.-T.; Chen, B.-Y.; Lin, M.-R.; Li, G.-Y. *Heterocycles* **2008**, 75, 2627–2648.
- (3) Sung, P.-J.; Chang, P.-C.; Fang, L.-S.; Sheu, J.-H.; Chen, W.-C.; Chen, Y.-P.; Lin, M.-R. *Heterocycles* **2005**, 65, 195–204.

- (4) Sung, P.-J.; Sheu, J.-H.; Xu, J.-P. *Heterocycles* **2002**, 57, 535–579.
- (5) Sung, P.-J.; Chen, M.-C. *Heterocycles* **2002**, 57, 1705–1715.
- (6) Jemal, A.; Siegel, R.; Xu, J.; Ward, E. *CA Cancer J. Clin.* **2010**, 60, 277–300.
- (7) Guruswamy, S.; Rao, C. V. *Gene Regul. Syst. Biol.* **2008**, 2, 163–176.
- (8) Janakiram, N. B.; Rao, C. V. *Acta Pharmacol. Sin.* **2008**, 29, 1–20.
- (9) Bowden, B. F.; Coll, J. C.; Vasilescu, I. M. *Aust. J. Chem.* **1989**, 42, 1705–1726.
- (10) Iwagawa, T.; Nishitani, N.; Nakatani, M.; Doe, M.; Morimoto, Y.; Takemura, K. *J. Nat. Prod.* **2005**, 68, 31–35.
- (11) Ishiyama, H.; Okubo, T.; Yasuda, T.; Takahashi, Y.; Iguchi, K.; Kobayashi, J. *J. Nat. Prod.* **2008**, 71, 633–636.
- (12) Wu, S.-L.; Sung, P.-J.; Su, J.-H.; Sheu, J.-H. *J. Nat. Prod.* **2003**, 66, 1252–1256.
- (13) (a) Hooft, R. W. W.; Straver, L. H.; Spek, A. L. *J. Appl. Crystallogr.* **2008**, 41, 96–103. (b) The Hooft method for determining absolute configuration uses Bayesian statistics to analyze the Bijvoet differences in a crystallographic data set. In Hooft's derivation, a model with the correct configuration should have a value near 0 for y , a value near 1 for $p_2(\text{true})$, a value near 1 for $p_3(\text{true})$, a value near 0 for $p_3(\text{twin})$, and a value near 0 for $p_3(\text{false})$. The p_2 value refers to the proposition that the model is either in the correct or incorrect configuration. The p_3 values refer to whether the model has the correct configuration, exhibits inversion or racemic twinning, or has the incorrect absolute configuration. The values for this sample are $y = -0.07(36)$, $p_2(\text{true}) = 0.988$, $p_3(\text{true}) = 0.768$, $p_3(\text{twin}) = 0.223$, and $p_3(\text{false}) = 0.009$. Thus we believe that the correct absolute configuration is shown in the model.
- (14) Raschke, W. C.; Baird, S.; Ralph, P.; Nakoinz, I. *Cell* **1978**, 15, 261–267.
- (15) Mather, J. P.; Roberts, P. E. *Introduction to Cell and Tissue Culture: Theory and Technique*; Springer: New York, 1998; p 66.